Effect of Intermediate Aerodisk Mounted Sharp Tip Spike on the Drag Reduction over a Hemispherical Body at Mach 2.0

Payal V. Tembhurnikar
Engineering Student
Department of Aeronautical Engineering
AnnaSaheb Dange College of Engineering & Technology, Ashta
India

Akash T. Jadhav
Engineering Student
Department of Aeronautical Engineering
AnnaSaheb Dange College of Engineering & Technology, Ashta
India

Devabrata Sahoo
Associate Professor
Department of Aeronautical Engineering
AnnaSaheb Dange College of Engineering & Technology, Ashta
India

Reduction of forebody drag in high speed flying vehicles such as rockets and missiles are of high research interest in the present time. In the present research, drag reduction obtained by using an intermediate aerodisk mounted sharp tip spike has been investigated using computational studies at Mach number of 2.0. The flowfield over a hemispherical blunt body with an intermediate aerodisk mounted sharp tip spike is investigated at zero degree angle of attack and the amount of drag reduction obtained is then compared with that of a conventional sharp tip spike mounted hemisphere. The presence of an intermediate aerodisk changes the flow physics and shock system over the blunt body. The change in the system of shock waves by mounting an intermediate aerodisk results in a higher percentage (20% higher) of drag reduction generated by the blunt spiked body moving at a supersonic speed of Mach 2.0. Use of intermediate aerodisk proves to be benificial in terms of drag reduction for spike lengths ranging beyond the critical length.

Keywords: *Supersonic flow, Drag reduction, Spike, Aerodisk.*

1. INTRODUCTION

The study of spike mounted blunt body moving at high-speed has gained the interest of researchers since past couple of decades. The major advantage of adding a spike on a blunt body moving at supersonic speed is its ability to change the flow physics and thereby reduce the forebody drag [1]. By mounting the spike on the stagnation point of a blunt body, the strong detached bow shock wave formed ahead of the body is replaced by a system of weaker shocks (leading edge shock, and reattachment shock). Also, a recirculation region is formed around the spike-forebody interface which is separated from the external flow by a shear layer. Figure 1 shows the schematic of the change in flow physics over a hemispherical body while mounting a typical spike. As a consequence of formation of weaker oblique shock waves, the pressure level over the blunt body surface reduces. This decrease in the pressure level thereby reduces the drag coefficient experienced by the blunt forebody. Previous researchers have already reported the reduction of drag force experienced by a blunt body moving at high speed by mounting of spike [2]. In addition, the recent review paper of Huang et al. [3] gives a detailed list of different research carried out over spike mounted blunt bodies moving at high speed. Various parametric studies on spike mounted hemispherical bodies related to drag reduction have also been reported in the recent past [4-10]. With increasing the spike length up to a critical length, the amount of drag reduction has been reported to increase [4]. As per Jones [4], for a hemispherical body moving at a Mach number of around 2.00, the spike length to main body diameter ratio (L/D) of the critical spike length providing maximum amount of drag reduction was reported to be L/D=1.5 (where, L is the spike length and D is the main body diameter). Later, researchers reported a further increase in amount of drag reduction in comparison to sharp tip spike by mounting an aerodisk at the spike tip location [11-14]. On mounting the aerodisk, an increase in the size of the recirculation zone is observed which thereby reduces the reattachment shock strength. This reduces the level of the surface pressure and hence a reduction in drag coefficient in obtained. Recently, Yadav et al. [15-16] using computational studies reported an even further increase in the amount of drag reduction at hypersonic flow by mounting a series of aerodisk along the spike stem in comparison to a single aerodisk mounted spiked body configuration. In addition to the spiked blunt bodies, numerous studies have also been conducted involving the investigation of the aerodynamic forces over more streamlined bodies (Cone and Ogive) without mounting any spike [17-19]. However, the focus of the present research is on spiked blunt bodies and all the above mentioned studies concentrating on the enhancement of the drag reduction over spiked blunt bodies moving at high-speed are conducted within the critical length of the spike.

In the present research, 2D axisymmetric computational studies have been conducted adopting k-ω turbulence model, to acquire the steady-state flow field over the hemispherical body mounted with sharp tip spikes of various lengths at freestream supersonic flow of Mach 2 and zero degree angle of attack. The flowfield obtained around the hemispherical body by mounting a sharp tip spike of critical spike length is compared with the one ob-

Received: April 2020, Accepted: June 2020
Correspondence to: Dr Devabrata Sahoo
Associate Professor, AnnaSaheb Dange College of Engineerng and Technology, Ashta, India – 416301
E-mail: devtapu@gmail.com
doi: 10.5937/fme2004779T

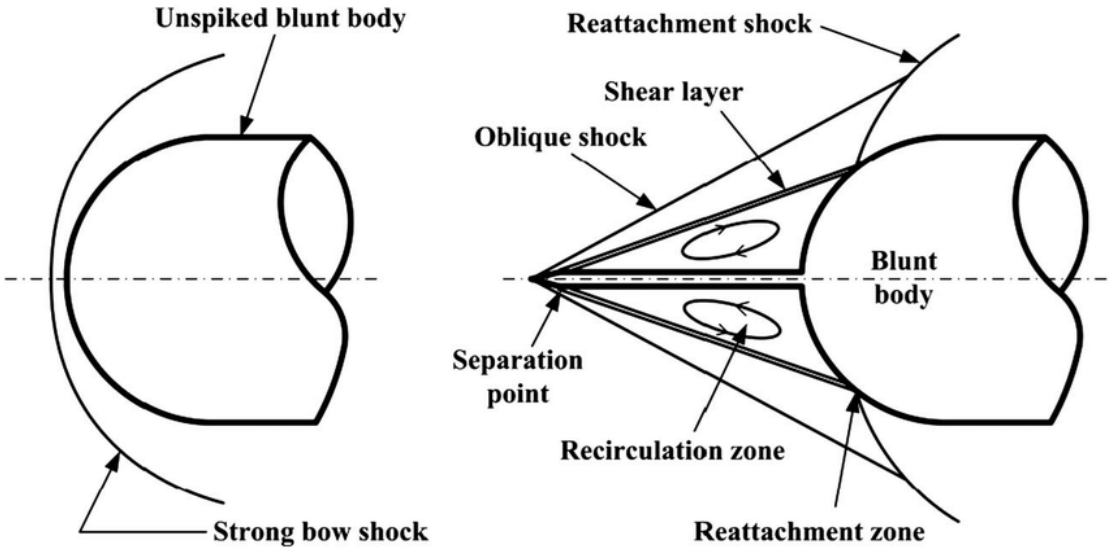

Figure 1 Schematic showing the flowfield over a clean and spiked hemisphere moving at supersonic speed.

tained by mounting a spike of length longer than the critical limit. Furthermore, an attempt is made to increase the percentage of drag reduction on a spike length beyond the critical limit by utilizing the information provided by Jones [4] and Yadav et al. [15-16].

An intermediate aerodisk is mounted over the spike stem of the sharp tip spike longer than the critical spike length and the flowfield generated over the spiked blunt body is captured and analyzed. The effect of the above mentioned spike on the amount of drag reduction is obtained and compared with that obtained by a conventional sharp tip spike.

2. GEOMETRY

A blunt hemispherical body with a main body diameter (D) of 15 mm and length of 1.5D has been used in the present study. All the spikes adopted have a sharp tip with half-cone angle of 10 degrees and a basic spike stem diameter of 2 mm (0.12D). Two different spike lengths (critical length, L/D=1.5 and beyond critical length, L/D=2.0) have been adopted to obtain the effect in the flowfield by increasing the spike length beyond critical length.

Further, in order to reduce the amount of drag reduction for the spiked body configuration with a spike of length beyond the critical length (L/D=2.0), an intermediate aerodisk is mounted on the spike stem. The geometry of the intermediate aerodisk used in the present investigation is adopted with reference to the aerodisk used by Yadav et al. [15-16]. The point of flow separation over the spike length for longest spike (L/D=2.0) has been considered as the location of mounting the intermediate aerodisk. The details of the spike and blunt body configurations adopted in the present study can be seen in Figure 2.

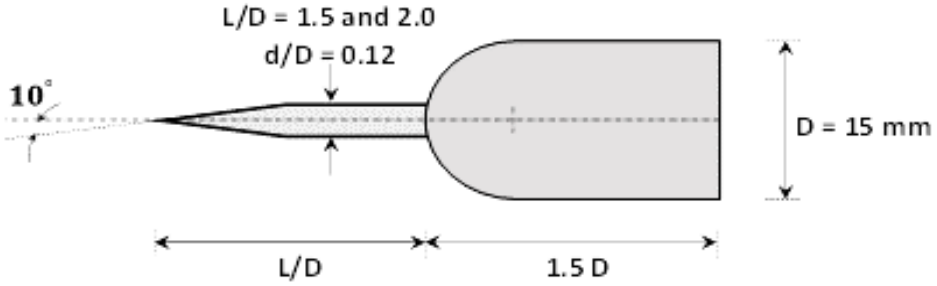

(a) Hemispherical body configuration with sharp spike

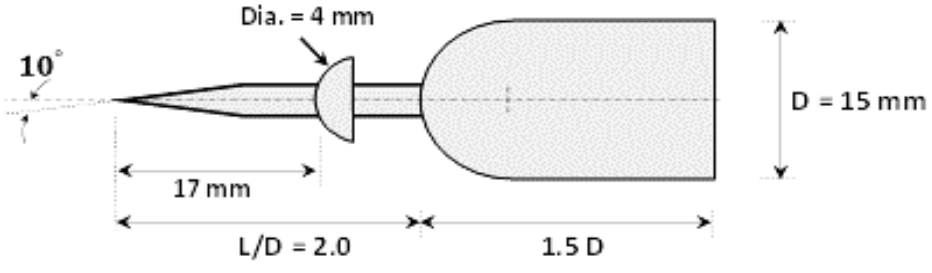

(b) Hemispherical body configuration with sharp spike and intermediate aerodisk

Figure 2 Geometry of the models adopted in the present study

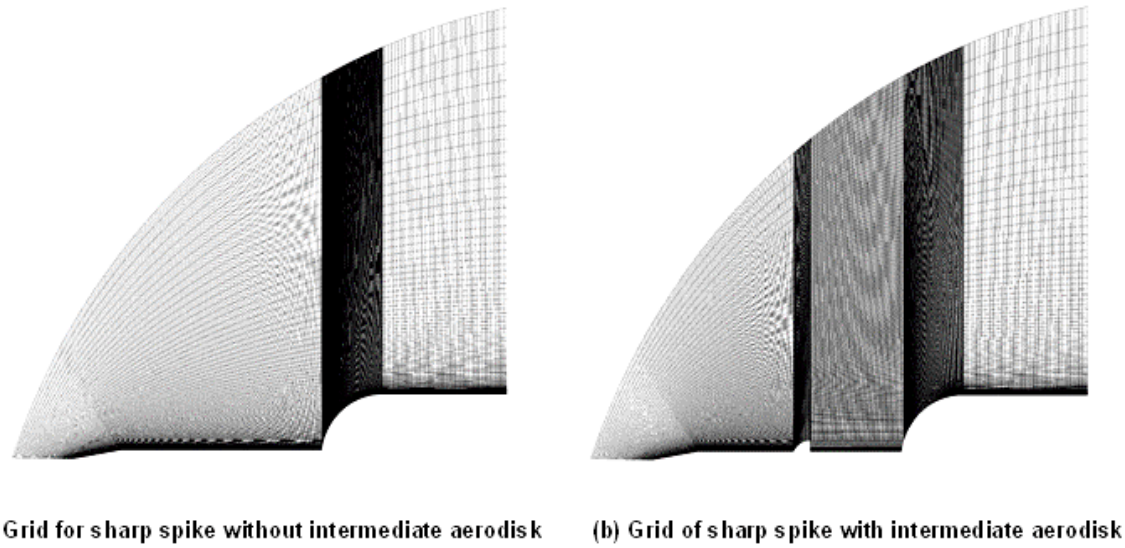

(a) Grid for sharp spike without intermediate aerodisk (b) Grid of sharp spike with intermediate aerodisk

Figure 3 Grids used in the present study for steady 2D axisymmetric computations

3. COMPUTATIONAL METHODOLOGY

In the present study, 2D axisymmetric steady-state computations have been performed at a freestream Mach Number of 2.0 and Reynolds Number of 3.5 x 10^5 (based on forebody diameter, D). The computations are carried out using the commercial CFD tool ANSYS-FLUENT, which uses a finite volume approach to solve the compressible Reynolds-Averaged Navier–Stokes (RANS) equations. The computations have been conducted adopting explicit coupled solver and using "k-ω" turbulence model. The use of this turbulence model has been decided by referring to the turbulence modeling exercise performed by Sahoo et al. [8] which reported "k-ω" turbulence model to be suitable for flow analysis over spiked bodies. A typical domain and mesh was finalized after making essential grid sensitivity tests, and obtaining a good match with the results reported in literature which is reported in the subsequent solver validation section.

Structured grids with uniform quadrilateral cells have been adopted having a first cell distance of the order of 1.0x10^3 mm. Based on the fine mesh near the wall, the y^+ value throughout the spiked body was of the order of 1.0. Photograph of the grids used in the current study are shown in Figure 3. The grids near the wall have been provided with necessary clustering for capturing the flow field precisely. The general grid size for present 2D axisymmetric computations is taken to be of the order of 90000 cells. The inlet has been specified by the pressure farfield boundary condition whereas no slip wall boundary conditions have been imposed on the main body and spike. The computational domain, overall grid and the boundary conditions adopted in the present research is shown over the validation spiked body model reported in [20] and can be seen in Figure 4. The purpose of preparing the grid and conducting simulation over the model reported by White [20] is to validate the mesh and the solver used in the present investigation. The details of the validation results is discussed in the next section. Furthermore, during the simulations, the residuals of the continuity and turbulent kinetic energy were monitored and the results were analyzed only once the residuals were converged to an order of 10^5.

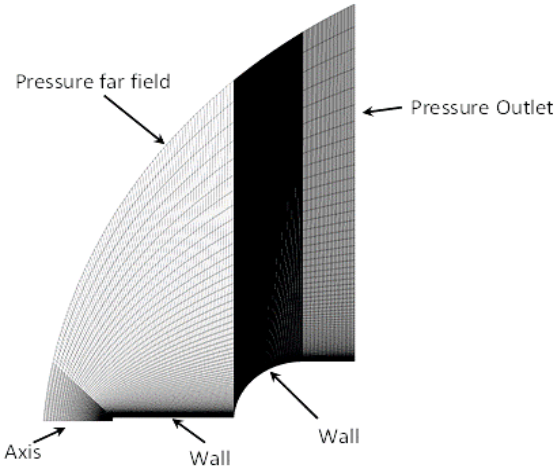

Figure 4 Flow domain and boundary types used in the present study

4. SOLVER VALIDATION

The result reported in [20] on a blunt body with spike having a spike length of L/D=0.875 at M=2.23 has been utilized for solver validation and to get a suitable grid. The blunt body is hemispherical in shape and the spike is having a flat tip. The geometrical detail of the model used for validation is shown in Figure 5. The computational domain and grid adopted for conducting computations over the validation model has been already presented in the previous section (Figure 4). The flowfield over the validation model has been simulated by using "k-ω" turbulence model and the result has been obtained in order to validate the solver. The time-averaged surface pressure distribution computed over the hemisphere has been compared with the measured time-averaged surface pressure distribution reported in White [20]. The comparison is presented in Figure 6. It can be clearly observed that the time-averaged pressure distribution derived from the present steady-state compu-

tation matches fairly with the reported experimental results, thus validates the grid and simulating tool.

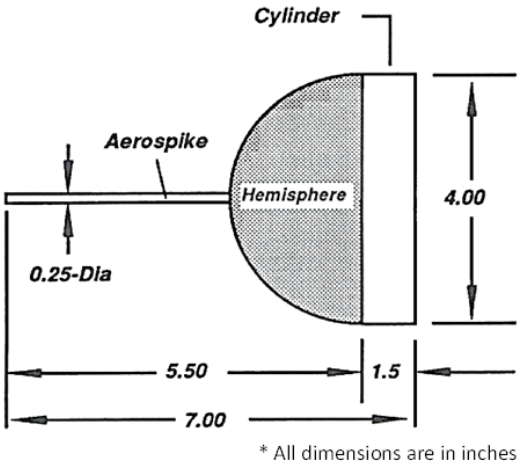

Figure 5 Geometrical detail of the reference model adopted for validation. [White, 1992]

5. RESULTS AND DISCUSSION

Computations have been performed at freestream Mach 2.0 flow to capture the flowfield over the spike mounted hemispherical blunt body. Sharp tip spike of L/D ratio 1.5 and 2.0 are adopted and the results are compared. The change in the amount of drag reduction by increasing the spike length beyond the critical length is found to be consistent with the previous reports. As reported by Jones [4], the amount of drag reduction is observed to be reducing if the spike length is increased from L/D=1.5 (critical length for Mach 2.0) to L/D=2.0. The comparison is shown at the later stage of this section. To accomplish the objective of enhancing the amount of drag reduction for spike with a length beyond the critical length, an intermediate aerodisk is mounted on the spike stem. The location for mounting the intermediate aerodisk is obtained from the computational result obtained for the case a hemispherical blunt body mounted with a conventional sharp tip spike of L/D=2.0. The location on the spike stem where the flow separates is considered to be the location for mounting the intermediate aerodisk. The idea of mounting the aerodisk at the point of separation is adopted from the basic concept of rising the separation point and increasing the size of recirculation region thereby reducing the drag value [11-14].

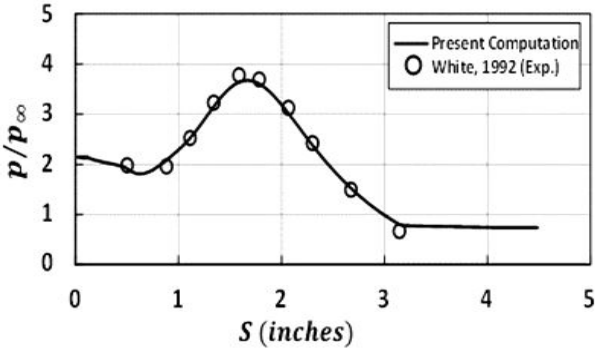

Figure 6 Comparison of time-averaged surface pressure distribution over the spiked hemisphere

The results of the computation performed over a sharp tip spike of L/D=2.0 mounted on a blunt hemisphere has been presented in Figure 7. It shows the density gradient contour overlapped with the time-averaged surface pressure distribution over the spike and the hemispherical blunt body.

From the density gradient contour shown in Figure 7, the flow features developed over the sharp tip spike can be clearly observed. The weak leading edge shock and the separation shock can be seen to generate from the spike tip and the spike stem, respectively. The expansion fan is also seen to generate at the spike tip shoulder location. In addition, the reattachment shock formed over the hemispherical body at the point of flow reattachment is also observed. The computed time-averaged surface pressure distribution is overlapped over the density gradient contour in order to justify our qualitative results. From the pressure distribution plot, it can be clearly seen that pressure rise occurs at three different locations which exactly corresponds to the locations where the three different shock waves are generated (leading edge, separation and reattachment shock). From Figure 7, the location of flow separation point over the spike stem is observed to be 17 mm from the spike tip. This location is then considered to mount the intermediate aerodisk to accomplish the objective of the present research.

Further 2D axisymmetric computations are conducted at Mach 2.0 over the blunt body mounted with a spike having a sharp tip with and without intermediate aerodisk and the results obtained are analyzed and compared. Density contours obtained from the present computations carried out over the different spiked body geometries are presented in Figure 8. The flowfield developed by increasing the spike length beyond the critical length and by mounting an intermediate aerodisk are compared in Figure 8.

On comparison of the density contours obtained over the hemisphere mounted with sharp tip spike of L/D=1.5 (Figure 8a) and L/D=2.0 (Figure8b), it can be clearly seen that the point of reattachment location does not change which change in the spike length beyond the critical length (L/D=1.5). As a result the reattachment shock strength remains same for these two cases (Figure8a and 8b). This is clearly observed from the color map of the density contours.

On adding an intermediate aerodisk at the flow separation point of the longer spike (L/D=2.0), the flow physics is observed to be changed (Figure 8c). It is observed that on mounting of an intermediate aerodisk, the separation point raises vertically upward thereby shifting the reattachment point downstream. The downstream shift in the reattachment point is shown in Figure 8 by vertical dashed line. This shift in the point of reattachment thus reduces the local flow turn angle at the reattachment point thereby reducing the strength of the reattachment shock. The reduction of the reattachment shock strength can also be observed clearly on comparing the shock wave through the color map of the density contours.

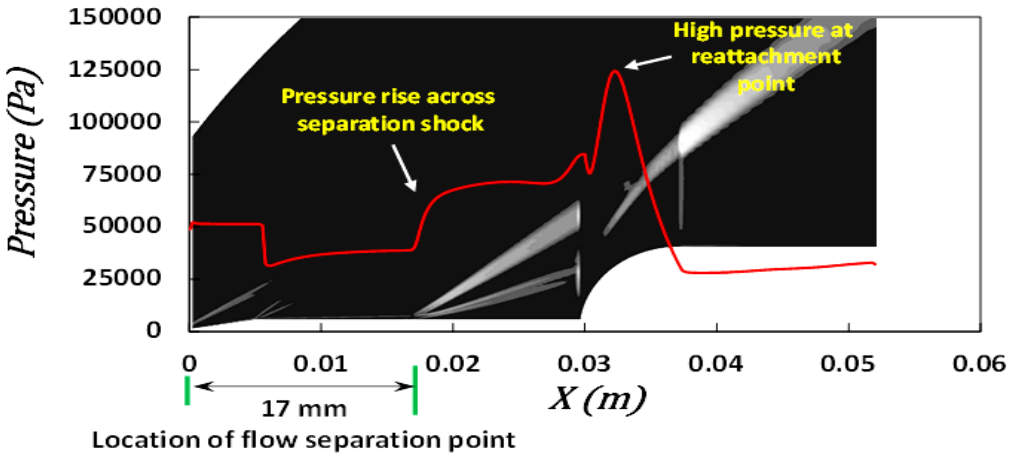

Figure 7 Computed density gradient contour overlapped with the computed time-averaged surface pressure distribution over the spiked hemisphere (L/D=2.0). Flow is from left to right.

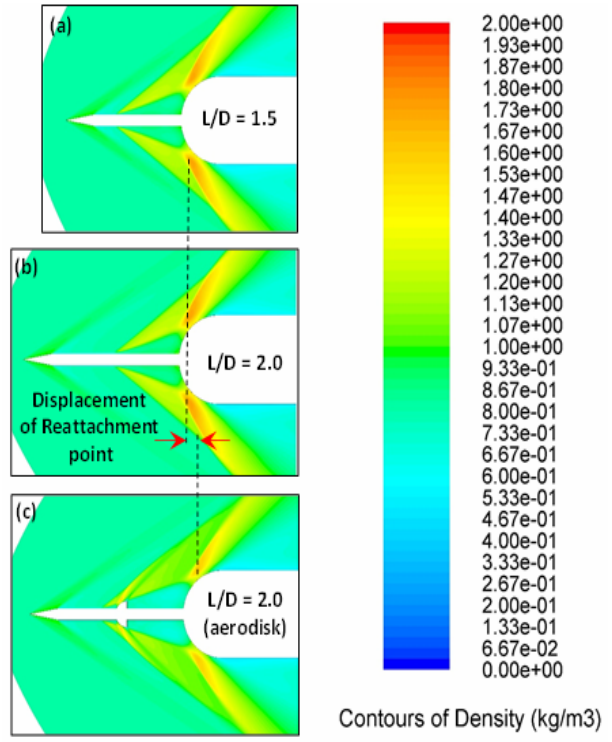

Figure 8 Density contour obtained over blunt hemisphere mounted with spike of various length and spike with intermediate aerodisk at supersonic flow of Mach 2.0. Flow is from left to right.

A detailed qualitative flow comparison using the computed density contours over the sharp tip spike cases of L/D=2.0 with and without intermediate aerodisk is shown in Figure 9a and 9b. As discussed in the previous paragraph, the increase in the size of recirculation region by mounting an intermediate aerodisk can be clearly observed in Figure 9b. In addition, the reduction in the flow turn angle (from ~ 44° to ~ 34°) and decreased reattachment shock strength can also be observed from the comparison of the density contour shown in Figure 9a and 9b.

As a result of the reduction in the reattachment shock strength by mounting of an intermediate aerodisk, the level of time-averaged surface pressure distribution can be expected to reduce. This reduction in the pressure level will thereby result in a further reduction on the value of drag coefficient by mounting an intermediate spike and hence an improved drag reduction can be achieved beyond the critical spike length.

To complete the hypothesis made in the previous paragraph with the help of the qualitative results, a detailed quantitative result analysis is also required. For that purpose the computed time-averaged surface pressure distribution of the forebody geometry for all the cases investigated in the present research are obtained and compared. The comparison is presented in Figure 10. From the comparison of the surface pressure distribution shown in Figure 10, the shift in the reattachment point location can be clearly observed. This shift in the reattachment point reduces the shock strength as already discussed and hence a decrease in the level of the pressure peak value is observed as expected from the qualitative analysis.

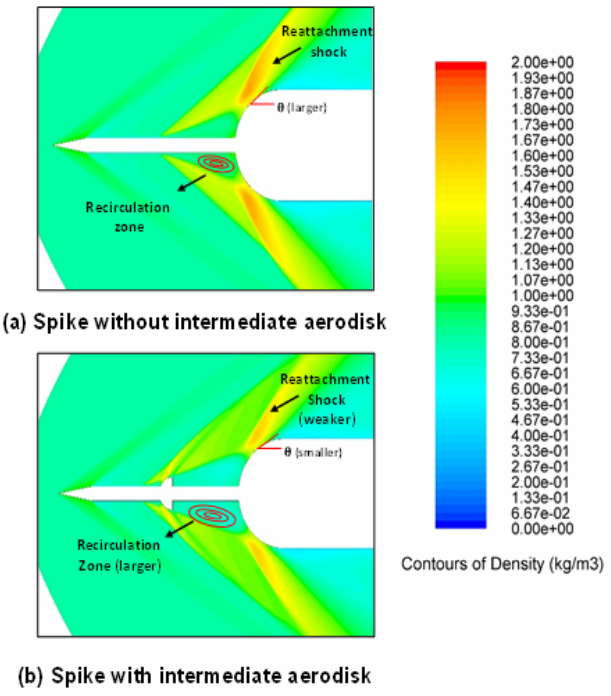

Figure 9 Comparison of computed density contour between sharp tip spike without and with intermediate aerodisk at supersonic flow of Mach 2.0. Flow is from left to right.

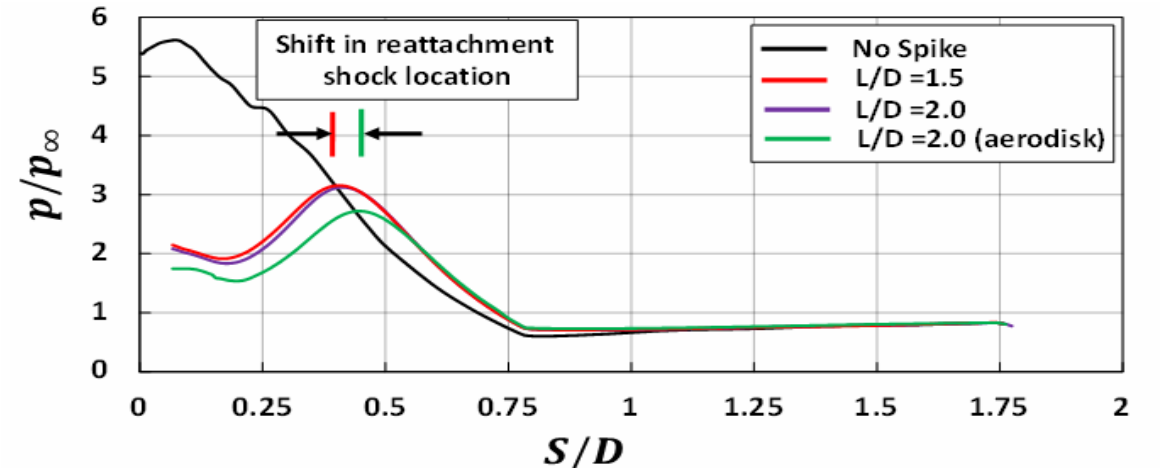

Figure 10 Comparison of the computed time-averaged surface pressure distribution over hemispherical forebody for different spiked body geometries investigated at supersonic flow of Mach 2.0.

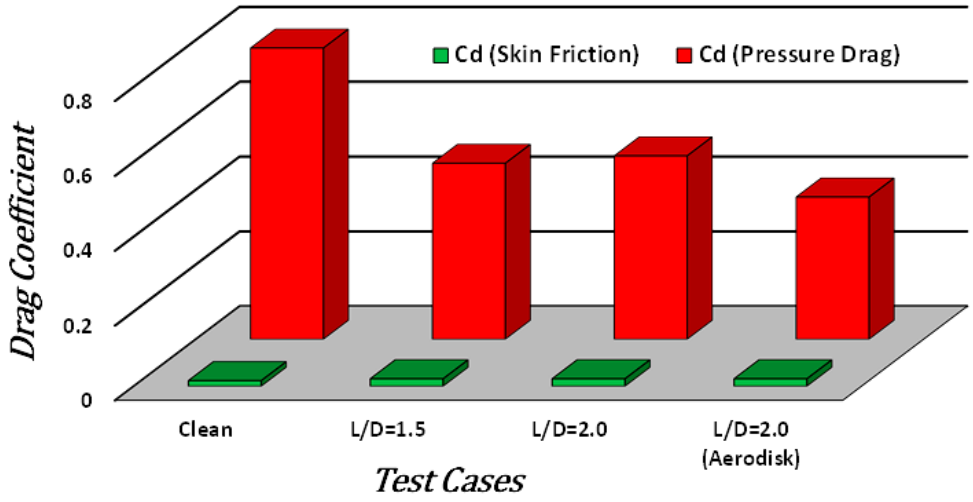

Figure 11 Computed drag coefficient values (skin friction drag and pressure drag) experienced by different spiked body configurations investigated in the present research.

Table 1 Computed total forebody drag coefficient values for different geometries considered in the present investigation.

Body	Cd (Pressure)	Cd (Skin Friction)	Cd (Total)
Clean	0.778	0.015	0.79
L/D=1.5	0.47	0.02	0.49
L/D=2.0 (Without Aerodisk)	0.49	0.02	0.51
L/D=2.0 (With Aerodisk)	0.38	0.02	0.40

This reduction in the level of pressure value is also clearly observed from the pressure plot for the case of sharp tip spike with intermediate aerodisk (green line). Also on comparison of the pressure distribution obtained for spike of L/D=1.5 and 2.0 (red and purple line, respectively), the change in the pressure level is observed to be minimal which is consistent with the previous reports [4]. From the analysis of the computed pressure distribution for the different cases under consideration, it can be expected that the amount of drag reduction marginally decreases on extending the spike length beyond the critical length to L/D=2.0. However, if an intermediate aerodisk is mounted at a suitable location over the spike stem, the amount of drag reduction can be expected to be enhanced even on the spike length beyond the critical limit.

The computed drag coefficient experienced by the different spiked body geometries investigated in the present research are obtained and presented in Table 1. It can be clearly observed from the table that the amount of drag reduction is further increased on mounting of the intermediate aerodisk on a sharp tip spike of length longer than the critical length

Furthermore, as it can be observed from Table 1, the total forebody drag coefficient values are a combination of the drag values contributed from the skin friction drag and the pressure drag. In order to find the individual contribution of both the major types of drag, the skin friction drag is calculated by integrating the wall shear stress distribution on the spiked blunt body and the pressure drag is calculated by integrating the pressure forces on the spiked blunt body. The whole

matrix of drag coefficient values experienced from the pressure drag as well as skin friction drag has been plotted in Figure 11 to have a better understanding. It can be clearly seen from Figure 11 that the skin friction drag remains almost unchanged with the change in the spike geometry. The major contribution in the change in the overall drag coefficient due to the change in spike geometry is by the pressure drag. This further justifies our findings which states the change in the pressure distribution is basically due to the change in the strength of the reattachment shock.

6. CONCLUSION

Computational study has been carried out at Mach number of 2.0 over hemispherical blunt body with sharp tip spike of various lengths. The flowfield and amount of drag reduction are found to remain unchanged on increasing the length of the sharp tip spike beyond the critical spike length. However, on mounting an intermediate aerodisk at the flow separation location over the spike stem for the case of spike length longer than the critical length, the flowfield is observed to change significantly. In the present investigation, the amount of drag reduction is observed to increase by almost 20% for the longer spike length (L/D=2.0) by mounting an intermediate aerodisk on the spike stem. It is observed that by mounting of an intermediate aerodisk on a longer spike (beyond critical spike length), the recirculation size increases thereby shifting the flow reattachment location downstream. This downward shift in the flow reattachment location reduces the local flow turn angle and hence results in a decrease in the reattachment shock strength. The reduction in the reattachment shock strength there by leads to a decrease in the pressure level and hence the fore body drag value is found to be further reduced. It has also been observed that the reduction is the overall drag is majorly from the pressure drag which is a result of the reduction in the reattachment shock strength on addition of the intermediate aerodisk. A detailed parametric study on the effect of the intermediate aerodisk geometry on the amount of drag reduction can be taken into future scope of research. The effect location of the intermediate aerodisk can also be considered for research in future.

REFERENCES

[1] Crawford, D. H.: Investigation of flow over a spiked nose hemisphere-cylinder at Mach number of 6.8, NASA-TN-D-118, 1959.

[2] Ahmed, M. Y.M. and Qin, N: Recent advances in the aerothermodynamics of spiked hypersonic vehicles, Progress of Aerospace Sciences, vol. 47, 425-499, 2011.

[3] Wei Huang, Zheng Chen, Li Yan, Bin-bin Yan and Zhao-bo Du: Drag and heat flux reduction mechanism induced by the spike and its combinations in supersonic flows: A review, Progress in Aerospace Sciences, vol. 105, 31-39, 2019.

[4] Jones J.: Flow Separation from Rods Ahead of Blunt Noses at Mach Number 2.72, NACA RM L52E05a, 1952.

[5] Yamauchi M., Fujii K., Higashino F.: Numerical Investigation of Supersonic Flow around a Spiked Blunt Body, Journal of Spacecraft and Rockets, vol. 32, no. 1, pp. 32–42, 1995.

[6] R. Kalimuthu, R.C. Mehta and E. Rathakrishnan.: Experimental investigation on spiked body in hypersonic flow, Aeronautical Journal, vol. 112 (1136), 593–598, 2008.

[7] Das S., Kumar P., Prasad J.K., Ralh M.K., and Rao R.K.M.: Drag Reduction of a Hemispherical Body adopting Spike at Supersonic Speed, Journal of Aerospace Science, vol. 65, no. 4, pp. 313–325, 2013.

[8] Sahoo D., Das S., Kumar P., and Prasad J.: Effect of spike on steady and unsteady flow over a blunt body at supersonic speed, Acta Astronautica, vol. 128, pp. 521–533, 2016.

[9] M. Ou, L. Yan, W. Huang, S.B. Li and L. Q. Li.: Detailed parametric investigations on drag and heat flux reduction induced by a combinational spike and opposing jet concept in hypersonic flows, International Journal of Heat and Mass Transfer, vol. 126, 10-31, 2018.

[10] Y. Xue, L. Wang, and S. Fu.: Drag reduction and aerodynamic shape optimization for spike-tipped supersonic blunt nose, Journal of Spacecraft Rockets, vol. 55 (3), 552-560, 2018.

[11] Menezes V., Saravanan S., Jagadeesh G., Reddy K.P.J.: Experimental investigations of hypersonic flow over highly blunted cones with aerospikes, AIAA Journal, vol. 41, no. 10, pp. 1955–1966, 2003.

[12] Milicev, S. S. and Pavlovic, D. M.: Influence of spike shape at supersonic flow past blunt nosed bodies: experimental study, AIAA Journal. Vol. 40, issue 5, 1018–1020, 2002.

[13] V. Kulkarni, V. Menezes and K.P.J. Reddy.: Effectiveness of aerospike for drag reduction on a blunt cone in hypersonic flow, Journal of Spacecraft Rockets, vol. 47 (3), 542–544, 2010.

[14] M.Y.M. Ahmed, N. Qin.: Drag reduction using aerodisks for hypersonic hemispherical bodies, Journal of Spacecraft Rockets, vol. 47 (1), 62-80, 2010.

[15] Yadav, R., Guven, U.: Aerothermodynamics of a hypersonic projectile with a double-disk aerospike, Aeronautical Journal, vol. 117, no. 1195, 913–928, 2013.

[16] Yadav, R. et al.: Aerothermodynamics of generic re-entry vehicle with a series of aerospikes at nose, Acta Astronautica, vol. 96, 1–10, 2014.

[17] Damljanović, D., Rašuo, B.: Testing of Calibration Models in Order to Certify the Overall Reliability of the Trisonic Blowdown Wind Tunnel of VTI, FME Transactions, Vol. 38, No. 4, pp. 167-172, 2010.

[18] Samardžić M., Isaković, J., Miloš, M., Anastasijević, Z., Nauparac D. B.: Measurement of the

Direct Damping Derivative in Roll of the Two Callibration Missile Models, FME Transactions, Vol. 41, pp. 189-194, 2013.

[19] Tarakka R., Salam, N., Jalaluddin, and Ihsan H.: Effect of Blowing Flow Control and Front Geometry Towards the Reduction of Aerodynamic Drag on Vehicle Models, FME Transactions, Vol. 47, pp. 552-559, 2019.

[20] White, J. T.: Application of Navier–Stokes Flowfield Analysis to the Aero-thermodynamic Design of an Aerospike-Configured Missile, AIAA, 0968, 1993.

УТИЦАЈ МЕЂУАЕРОДИСКА СА МОНТИРАНИМ ОШТРИМ ШИЉАСТИМ ВРХОМ НА СМАЊЕЊЕ ОТПОРА ПО ПОВРШИНИ ПОЛУЛОПТАСТОГ ТЕЛА ПРИ МАХОВОМ БРОЈУ 2.0

П.В. Тембурникар, А.Т. Јадав, Д. Сахо

Данас се велики број истраживача бави проблемом смањења отпора предњег дела летелица као што су ракете и пројектили. У овом раду је смањење отпора постигнуто коришћењем међуаеродиска са монтираним оштрим шиљастим врхом, компјутерским прорачуном при Маховом броју 2.0. Струјно поље по површини полулоптастог тупог тела са међуаеродиском је испитивано при нултом степену нападног угла и резултат смањења отпора је упоређен са резултатом добијеним код конвенционалног оштрог шиљастог врха монтираног на полулопти.

Присуство међуаеродиска мења физику протока и систем удара по површини тупог тела. Промена у систему ударних таласа монтирањем међуаеродиска смањује отпор (за 20%) који ствара тупо тело са шиљастим врхом при суперсоничној брзини од 2.0 Маха. Доказано је да коришћење међуаеродиска доводи до смањења отпора већег од критичне дужине шиљка.